

## Article

# Evaluating Wastewater Quality Parameters as an Alternative or Complement to Molecular Indicators for Normalization during SARS-CoV-2 Wastewater-Based Epidemiology

Judith Straathof <sup>1</sup> and Natalie M. Hull <sup>1,2,\*</sup> 

<sup>1</sup> Department of Civil, Environmental, and Geodetic Engineering, The Ohio State University, Columbus, OH 43210, USA; straathof.1@buckeyemail.osu.edu

<sup>2</sup> Sustainability Institute, The Ohio State University, Columbus, OH 43210, USA

\* Correspondence: hull.305@osu.edu or nataliehull@boisestate.edu

**Abstract:** Measuring fecal nucleic acid indicators for data normalization can increase costs during wastewater-based epidemiology (WBE). The efficacy of routinely assayed water quality parameters was assessed as an alternative or complement to fecal nucleic acid viral indicator data for their utility in adjusting measured SARS-CoV-2 gene concentrations to improve the relationship between wastewater molecular data and clinical COVID-19 case data. This research covers two study designs: grab samples collected from sewers serving The Ohio State University campus and composite influent samples collected at five wastewater treatment plants (WWTPs) across the state of Ohio. Weekly mandatory clinical testing was used to monitor infections in the student population, and statewide cases were reported through voluntary clinical testing. Statewide WWTP results showed significant strong correlation between SARS-CoV-2 concentrations in the wastewater and confirmed COVID-19 cases, and correlation increased when normalized by flow and additionally increased when normalized by pH, total suspended solids, and temperature, but correlation decreased when normalized by a nucleic acid fecal viral indicator (PMMoV). On campus, correlations were generally not significant unless normalized by PMMoV and/or UV absorbance parameters. Because water quality parameters are routinely assayed at wastewater treatment plants and some may be collected by autosamplers, incorporating wastewater quality data may improve WBE models and could minimize molecular and cellular testing for fecal indicators to decrease costs.

**Keywords:** COVID-19; wastewater biomarkers; normalization; dynamic population; wastewater characteristics analysis



**Citation:** Straathof, J.; Hull, N.M. Evaluating Wastewater Quality Parameters as an Alternative or Complement to Molecular Indicators for Normalization during SARS-CoV-2 Wastewater-Based Epidemiology. *Environments* **2024**, *11*, 80. <https://doi.org/10.3390/environments11040080>

Academic Editors: Qiuda Zheng and Zacharias Frontistis

Received: 22 February 2024

Revised: 28 March 2024

Accepted: 9 April 2024

Published: 12 April 2024



**Copyright:** © 2024 by the authors. Licensee MDPI, Basel, Switzerland. This article is an open access article distributed under the terms and conditions of the Creative Commons Attribution (CC BY) license (<https://creativecommons.org/licenses/by/4.0/>).

## 1. Introduction

Wastewater-based epidemiology (WBE) is an effective management tool for public health surveillance and decision making using wastewater measurements, including pharmaceuticals, antibiotic resistant genes, illicit drugs, and pathogens. During the COVID-19 pandemic, WBE became more widely used across the world to complement clinical tests of SARS-CoV-2 [1]. Clinical testing is costly and limited in tracking positive cases, especially when at-home tests are widely available and people with mild or no symptoms are unlikely to seek medical care. Since WBE does not rely on clinical testing, it allows for early detection of SARS-CoV-2 concentration changes within specific communities, as well as emerging variants [2]. This allows public health officials to make informed decisions to help prevent further spread or raise awareness for at-risk populations within specific communities.

Data normalization is used as a measurement correction to address variations in wastewater, such as fecal strength and dilution in the watershed, that can have an impact on the SARS-CoV-2 concentration in wastewater. Estimating the concentration of any biological or chemical marker in wastewater is complicated by flow changes and dilution events, the dynamic size of the population served, and the stability and transport mechanics

of the biomarker being monitored in the sewershed [3–6]. Although there is currently no consensus on which normalization parameter results in the strongest correlation between SARS-CoV-2 concentration in wastewater and COVID-19 cases, most approaches use population size, flow, and estimation of fecal strength [3,7–11].

The population within a sewershed can have fluctuations due to commuters, tourism, and part-time residents, which can make the use of census data for population size in a wastewater sewershed up to 50% inaccurate [12]. The population that a wastewater treatment plant (WWTP) serves can be estimated with a static number through census data, or population can also be estimated dynamically through influent flow, chemical parameters, mobile device data [8,13], or human fecal content.

Human fecal content, or fecal strength, has been estimated through biomarker organisms or compounds specific to human waste, such as Pepper Mild Mottle Virus (PMMoV), crAssphage, fecal coliforms, *Bacteroides* HF183, bacteriophages, etc., but using these to normalize correlations between cases and SARS-CoV-2 has not been consistent, with some studies reporting improved correlations and some studies reporting weakened or inconsistent correlations [7,9–11,14–16]. PMMoV is present in wastewater due to the consumption of peppers and related foods [17–19] and therefore is theorized to work as a correction for true fecal strength in surveys with large populations [20,21]. However, although PMMoV is found in high concentrations in wastewater, it can vary based on dietary, cultural, and socio-economic trends. For example, a positive relationship between temperature and PMMoV indicated a seasonal trend of pepper consumption, possibly due to changes in availability or prices [3]. Additionally, different WBE targets or indicators and their nucleic acids can differ in persistence, decay, extraction, and recovery efficiency [22,23], further compounded by the complex and variable wastewater matrices, which may inhibit the use of a fecal nucleic acid indicator. Total coliforms and *E. coli* have also been used as an indicator of human fecal waste presence, and they can also indicate the relative amount of human fecal content across samples [24,25].

Temperature, pH, organic matter, solids content, sewer residence time, sampling method, and microbial competition are known to have an influence on viral RNA fate and are assumed to have an impact on SARS-CoV-2 detection in wastewater [26–29]. A pH greater than 7.4 lowers the detection of SARS-CoV-2 [30], with maximum SARS-CoV-2 detection within a pH range of 7.1–7.4 [3,31] and undetected in wastewater with a pH greater than 8.8 [32]. Higher wastewater temperature also negatively impacts the detection of SARS-CoV-2 [33–36], which is especially important to take into account when sampling at locations with large temperature swings during winter and summer seasons. At 10 °C, the decay rate of SARS-CoV-2 in wastewater is already greater than at 4 °C [37], with it increasing as wastewater temperature increases [26]. Specific ultraviolet absorbance (SUVA or ultraviolet (UV) absorbance normalized by dissolved organic carbon (DOC)) is a measure of aromaticity and has been positively correlated with dissolved organic carbon hydrophobicity and molecular weight [38]. In addition to SUVA, ratios of UV absorbance at specific wavelengths can provide information on the structure and composition of DOC, such as its molecular weight, humification, or aromaticity [38]. SUVA and absorbance properties can be used to monitor wastewater treatment processes [39–41] and can differentiate wastewater sources [42], and relationships with WBE data have been explored [43]. However, these optical absorbance properties have not yet been evaluated for normalization to improve WBE relationships by accounting for the variable nature of organic matter. Normalizing for these parameters that impact SARS-CoV-2 in wastewater could aid in strengthening correlations to COVID-19 cases.

This study compares the correlation between COVID-19 cases and normalized and unnormalized SARS-CoV-2 concentrations in the auto-sampled WWTPs influent of five wastewater systems and grab-sampled sewer manholes from a university campus using multiple normalization approaches. Grab samples, especially ones close to their source, only capture a small snapshot of the flow in a sewer. Although 24 h composite samples with flow measurements are ideal, there could be instances where flow is difficult to measure,

such as when autosamplers are placed in sewers on campuses or in areas where resources or space are limited [44]. There are two different datasets to provide information about the two specific situations because different water quality parameters were measured for each case. While WBE is limited by variable SARS-CoV-2 shedding rates [45], accuracy of COVID-19 clinical data, testing accessibility, and test seeking behavior, exploring WBE correlations between SARS-CoV-2 and clinical data remains a common approach to evaluate normalization efficacy [46]. The objective of this study was to investigate alternative or complementary parameter(s) to molecular human fecal indicators (e.g., PMMoV) for normalizing SARS-CoV-2 gene concentrations in wastewater to improve correlations between SARS-CoV-2 in wastewater with COVID-19 cases.

## 2. Materials and Methods

### 2.1. Wastewater Samples Collection

#### Wastewater Treatment Plants

Wastewater samples were collected from wastewater treatment plants across the state as part of the Ohio Coronavirus Wastewater Monitoring Network [47]. In this study, results from five wastewater treatments plants [11] are further investigated. Influent composite wastewater samples (flow-proportionate, 24 h,  $n = 542$ ) were collected by autosamplers at Beaver Creek Water Resources Facility (WRRF), Eaton Wastewater Treatment Plant (WWTP), Greenville WWTP, Oxford WWTP, and Tri-Cities North Regional WWTP (Table 1). This study covers samples from 3 January 2021 to 29 June 2022 for Beaver Creek WRRF, Oxford WWTP, and Tri-Cities North Regional WWTP; from 1 August 2021 to 26 June 2022 for Eaton WWTP; and from 20 October 2021 to 29 June 2022 for Greenville WWTP. Eaton WWTP provided samples once a week and the other WWTPs provided samples twice a week. Samples were transported by courier from WWTPs to our lab on ice to minimize the effect of storage temperature on SARS-CoV-2 detection and processed immediately upon arrival.

**Table 1.** Average wastewater parameters for the five statewide WWTPs during the study  $\pm$  standard deviations.

| WWTP               | # of Samples (n) | Flow Rate (m <sup>3</sup> /day) | pH              | Temperature (°C) | TSS (mg/L)      | Population in Sewershed |
|--------------------|------------------|---------------------------------|-----------------|------------------|-----------------|-------------------------|
| Beaver Creek WRRF  | 140              | 34,990 $\pm$ 9584               | 6.32 $\pm$ 0.36 | 15.5 $\pm$ 2.75  | 152 $\pm$ 95.2  | 47,000                  |
| Eaton WWTP         | 48               | 5425 $\pm$ 2891                 | 7.58 $\pm$ 0.54 | 17.5 $\pm$ 3.23  |                 | 10,000                  |
| Greenville WWTP    | 64               | 10,148 $\pm$ 3350               | 7.63 $\pm$ 0.12 | 14.7 $\pm$ 2.59  | 87.6 $\pm$ 35.6 | 14,000                  |
| Oxford WWTP        | 140              | 6507 $\pm$ 3278                 | 7.49 $\pm$ 0.13 | 16.3 $\pm$ 3.55  | 276 $\pm$ 122   | 21,300                  |
| Tri-Cities NR WWTP | 140              | 40,496 $\pm$ 14,935             | 7.47 $\pm$ 0.13 | 17.0 $\pm$ 3.30  | 180 $\pm$ 174   | 65,000                  |

#### University Campus Sewer Samples

Wastewater grab samples were collected once a week from 1 September 2020 to 3 December 2020 from six wastewater sewer junctions on The Ohio State University (OSU) campus, capturing wastewater from dorms housing 7767 on-campus student residents (60% of total on-campus student residents) ( $n = 79$ ). Two bottles were collected at each site, with one bottle to test for molecular data and the other bottle to test wastewater characteristics. Samples were transported across campus to each lab on ice to minimize effect of storage temperature on SARS-CoV-2 detection. The six sites encompassed sewer flows from 19 dormitories, one recreational fitness facility, and three dining facilities. Further details of each site are described in Lu et al., 2022 [9].

### 2.2. Analytical Methods

#### 2.2.1. Molecular Methods

##### Wastewater Treatment Plants

N1 and N2 SARS-CoV-2 RNA genes and Pepper Mild Mottle Virus (PMMoV) were extracted from wastewater and quantified by reverse transcription quantitative polymerase

chain reaction (RT-qPCR). PMMoV was used as a viral human fecal indicator. Analysis was performed on RNA samples diluted by factors of 1:2, 1:5, 1:10, or 1:100 to minimize the impact of inhibition. The methods of sample processing from collection and upon arrival at the lab, RNA extraction, quantification, and data computation are described in detail in Ma et al., 2022 [11]. SARS-CoV-2 data are publicly available for these and other utilities on the Ohio Department of Health (ODH) COVID-19 Dashboard [48].

#### University Campus Sewer Samples

Digital droplet PCR (ddPCR) assays were used to quantify N1, N2, and E SARS-CoV-2 genes and PMMoV. Firefly (Coleoptera) Luciferase control RNA was used to detect PCR inhibition; none was detected [9]. The methods of sample processing from collection and upon arrival at the lab, RNA extraction, quantification, and data computation are described in detail in Lu et al., 2022 [9].

### 2.2.2. Physicochemical Characterization Methods

#### Wastewater Treatment Plants

The WWTPs provided influent flow volume over the composite sample 24 h collection period, pH, minimum and maximum temperature (Eaton WWTP provided an average temperature value), and total suspended solids (TSS) (Eaton did not provide TSS) as part of their routine monitoring (Table 1). Average temperature was calculated for the four WWTPs from the minimum and maximum temperatures values provided. Measurements were taken following standard procedures. Data are publicly available for these and other utilities on the ODH COVID-19 Dashboard [48].

#### University Campus Sewer Samples

Directly after sample collection while still at the sample site, field measurements were taken with a multiparameter meter (Hanna HI98194) for both sample bottles. The multiparameter meter was calibrated weekly according to manufacturer directions and using manufacturer-supplied solutions. The meter measured temperature, pH, electrical conductivity (EC), DOC, oxidation reduction potential (ORP), and pressure. Based on those values, it calculated total dissolved solids, resistivity, and salinity. These and other water quality data are shown in Table 2, Table 3 and Table S2. After field measurements were completed, samples were transported in a cooler with ice until storage in a 4 °C refrigerator until further processing the same day.

**Table 2.** Average wastewater parameters for the six campus sites during the study  $\pm$  standard deviations.

| Campus Site | # of Samples (n) | Turbidity (NTU) | pH              | Temperature (°C) | TSS (mg/L)    | Population in Dorms Served |
|-------------|------------------|-----------------|-----------------|------------------|---------------|----------------------------|
| 1           | 12               | 189 $\pm$ 210   | 8.47 $\pm$ 0.42 | 23.3 $\pm$ 2.76  | 493 $\pm$ 486 | 178                        |
| 2           | 14               | 231 $\pm$ 299   | 8.40 $\pm$ 0.36 | 22.7 $\pm$ 2.98  | 401 $\pm$ 353 | 1685                       |
| 3           | 12               | 192 $\pm$ 270   | 7.91 $\pm$ 0.57 | 22.6 $\pm$ 2.22  | 497 $\pm$ 719 | 3450                       |
| 4           | 14               | 169 $\pm$ 114   | 8.48 $\pm$ 0.23 | 22.2 $\pm$ 2.98  | 511 $\pm$ 335 | 872                        |
| 5           | 13               | 144 $\pm$ 47.2  | 6.63 $\pm$ 0.42 | 24.9 $\pm$ 2.89  | 218 $\pm$ 103 | 228                        |
| 6           | 14               | 115 $\pm$ 27.9  | 8.44 $\pm$ 0.19 | 21.9 $\pm$ 2.63  | 313 $\pm$ 106 | 1354                       |

*E. coli* and total coliforms were measured based on Hach Method 10029, USEPA approved. Broth ampules (m-ColiBlue24™ Broth Culture Media, M00PMCB24, Millipore-Sigma™, Burlington, MA, USA) were emptied onto sterile absorbent pads (Millipore-Sigma™ AP10045S0) in sterile petri dishes (VWR 25384-092). A 0.45  $\mu$ m membrane filter (Fisher Scientific 09-719-555, Waltham, MA, USA) was placed on a sterile membrane filter apparatus. *E. coli* were counted as blue colored colonies, while total coliforms were summed blue and red colored colonies.

**Table 3.** Average organic and optical wastewater parameters for the six campus sites during the study  $\pm$  standard deviations. See Table S1 for wavelengths of absorbance ratios.

| Site | DOC (mg/L)      | SUVA 254                      | SUVA 280                                    | SUVA 400                                    | E2:E3           | <sup>a</sup><br>E2:E4 | <sup>b</sup><br>E2:E4 | <sup>c</sup><br>E2:E4 | <sup>a</sup><br>E4:E6 | <sup>b</sup><br>E4:E6 | <sup>c</sup><br>E4:E6 | <sup>d</sup><br>E4:E6 |
|------|-----------------|-------------------------------|---|---|-----------------|-----------------------|-----------------------|-----------------------|-----------------------|-----------------------|-----------------------|-----------------------|
| 1    | 93.6 $\pm$ 44.8 | 0.02 $\pm$ 8 $\times 10^{-3}$ | 0.02 $\pm$ 6 $\times 10^{-3}$               | 7 $\times 10^{-3}$ $\pm$ 3 $\times 10^{-3}$ | 3.46 $\pm$ 0.51 | 5.95 $\pm$ 1.37       | 4.17 $\pm$ 1.15       | 6.55 $\pm$ 1.41       | 3.72 $\pm$ 0.34       | 4.39 $\pm$ 0.51       | 4.70 $\pm$ 0.55       | 4.86 $\pm$ 0.74       |
| 2    | 135 $\pm$ 64.8  | 0.01 $\pm$ 7 $\times 10^{-3}$ | 0.01 $\pm$ 5 $\times 10^{-3}$               | 4 $\times 10^{-3}$ $\pm$ 1 $\times 10^{-3}$ | 3.61 $\pm$ 1.38 | 6.52 $\pm$ 2.83       | 5.05 $\pm$ 2.46       | 7.37 $\pm$ 3.33       | 3.94 $\pm$ 0.73       | 4.72 $\pm$ 1.59       | 4.74 $\pm$ 1.07       | 5.13 $\pm$ 1.56       |
| 3    | 81.1 $\pm$ 41.4 | 0.02 $\pm$ 6 $\times 10^{-3}$ | 0.01 $\pm$ 5 $\times 10^{-3}$               | 6 $\times 10^{-3}$ $\pm$ 2 $\times 10^{-3}$ | 3.33 $\pm$ 0.46 | 5.50 $\pm$ 0.80       | 4.18 $\pm$ 1.22       | 5.96 $\pm$ 0.86       | 3.84 $\pm$ 0.49       | 4.65 $\pm$ 0.78       | 4.79 $\pm$ 0.63       | 4.94 $\pm$ 1.03       |
| 4    | 102 $\pm$ 28.7  | 0.01 $\pm$ 4 $\times 10^{-3}$ | 0.01 $\pm$ 4 $\times 10^{-3}$               | 5 $\times 10^{-3}$ $\pm$ 2 $\times 10^{-3}$ | 3.37 $\pm$ 0.45 | 5.64 $\pm$ 0.78       | 4.32 $\pm$ 0.95       | 6.09 $\pm$ 0.80       | 3.88 $\pm$ 0.20       | 4.82 $\pm$ 0.66       | 5.03 $\pm$ 0.73       | 5.07 $\pm$ 0.99       |
| 5    | 213 $\pm$ 90.1  | 0.00 $\pm$ 2 $\times 10^{-3}$ | 9 $\times 10^{-3}$ $\pm$ 2 $\times 10^{-3}$ | 2 $\times 10^{-3}$ $\pm$ 9 $\times 10^{-4}$ | 3.74 $\pm$ 0.60 | 7.13 $\pm$ 2.41       | 5.27 $\pm$ 2.14       | 8.85 $\pm$ 5.58       | 4.18 $\pm$ 0.43       | 4.67 $\pm$ 1.10       | 4.67 $\pm$ 1.09       | 4.82 $\pm$ 0.97       |
| 6    | 91.5 $\pm$ 26.9 | 0.01 $\pm$ 6 $\times 10^{-3}$ | 0.01 $\pm$ 4 $\times 10^{-3}$               | 5 $\times 10^{-3}$ $\pm$ 1 $\times 10^{-3}$ | 3.64 $\pm$ 0.50 | 6.13 $\pm$ 0.78       | 4.69 $\pm$ 1.14       | 6.76 $\pm$ 0.92       | 3.88 $\pm$ 0.57       | 4.53 $\pm$ 0.91       | 4.61 $\pm$ 0.77       | 4.99 $\pm$ 1.23       |

Turbidity measurements (three replicates for each sample) were taken according to American Public Health Association (APHA) standard method 2130B. The Mirco 100 Turbidimeter (HF scientific, Inc., Fort Myers, FL, USA) was used. The sample bottle was inverted for 30 s before measurement to resuspend solids.

Total suspended solids (TSS) were measured according to APHA standard method 2540D. Glass fiber filter disks (Hach 253000, Loveland, CO, USA) with a size of 0.7 mm were used along with aluminum weighing dishes (Fisherband, 08-732-102, Waltham, MA, USA).

Dissolved organic carbon (DOC) was measured according to the APHA standard 5310B combustion–infrared method and the instrument manual in a Shimadzu TOC-V<sub>CSN</sub> analyzer (638-91062-02, Kyoto, Japan). Clear borosilicate glass bottles were washed with DI three times, sealed with aluminum foil, and baked at 550 °C for at least 4 h to destroy trace carbon. Samples were inverted for 30 s and then 8 mL of sample was combined with 24 mL of DI and filtered through a 0.45  $\mu$ m polypropylene membrane syringe filters (Foxy Life Sciences, 37B-3216-OEM, Salem, OR, USA) that were pre-rinsed with DI. Four replicates of each sample bottle were measured. DI water was measured between each sample type. The instrument was set to complete a 50  $\mu$ L injection of each sample cell three times, two-minute sparging time, and 2.0% acid injection. The instrument was calibrated monthly using a potassium phthalate, potassium nitrate, and hydrogen chloride stock solution.

Starting in October, ultraviolet (UV) absorbance was measured at 250, 252, 254, 280, 365, 400, 436, 450, 452, 460, 465, 600, 650, 660, and 665 nm with a disposable UVette (Eppendorf, 952010077, Hamburg, Germany) and Uvette adapter in the ThermoScientific NanoDrop 2000c Spectrophotometer (Waltham, MA, USA). DI water was used to blank the instrument and the Uvette was rotated so that the measurement pathlength was 2 mm. SUVA was calculated by dividing the absorbance at a specific wavelength by the dissolved organic carbon concentration. SUVA<sub>254</sub> [49], SUVA<sub>280</sub> [50], and SUVA<sub>400</sub> [51] were calculated. In addition to SUVA, other ratios between UV absorbance at specific wavelengths which can relate to organic matter properties were calculated [52–59]. Table S1 in the Supplementary Materials (SM) lists the different ratios.

### 2.3. Human Case Data

#### Wastewater Treatment Plants

Daily total number of positive COVID-19 cases from voluntary testing for each individual sewershed were obtained from the ODH COVID-19 Dashboard [48]. The 7-day moving average was calculated as previously [10,11]. For the pooled dataset, the 7-day moving average was also normalized by the population of each sewershed using the static population number (Table 1). Case data are summarized in Ma et al., 2022 [11] and the ODH COVID-19 Dashboard [48].

#### University Campus Sewer Samples

Daily total numbers of positive COVID-19 cases for campus during mandatory testing were obtained from the OSU COVID-19 Dashboard [60]. Case data were only available for all on-campus residents, including students living in dormitories whose sewer systems were not captured by this study. Therefore, case data could not be correlated directly to individual collection sites. Instead, SARS-CoV-2 concentrations were combined into a weighted sum per week across sites based on the ratio of the contributing population

per site to the total population sampled. This weekly weighted SARS-CoV-2 sum was correlated to the COVID-19 cases 7-day moving average (final  $n = 14$  for the semester). The 7-day moving average correlated more strongly to SARS-CoV-2 concentrations than the 14-day moving average. These and other campus case data are summarized in Lu et al., 2022 [9].

#### 2.4. Statistical Analysis

Spearman correlations were calculated between 7-day moving averages of positive COVID-19 cases and either all unnormalized gene concentrations of SARS-CoV-2 or all normalized concentrations. The expectation is that parameters that indicate dilution or contribute to a lower detection of SARS-CoV-2, such as flow or temperature, can be corrected for by multiplying SARS-CoV-2 gene concentrations by said parameters, while parameters that indicate an increased concentration of SARS-CoV-2, such as human fecal indicators or total suspended solids, can be corrected for by dividing SARS-CoV-2 by said parameters. Because the impact of some water qualities is unknown, we tested both division and multiplication normalization of water quality parameters. Normalization was done through dividing and multiplying SARS-CoV-2 concentration by all wastewater quality parameters measured (Equations (S1)–(S128) in SM). SARS-CoV-2 concentration was also divided by the PMMOV concentration and normalized further by dividing and multiplying it with the wastewater quality parameters. For the WWTs, flow was measured. Therefore, SARS-CoV-2 concentrations were multiplied by flow, including the SARS-CoV-2 concentrations normalized by PMMOV concentrations. This was then divided and multiplied by the wastewater quality parameters.

Spearman correlations were calculated using the function `rcorr()` in Rstudio V. 3.6.3. Spearman's  $\rho$  values were interpreted as follows: strong correlation had a  $\rho$ -value  $> 0.7$ ; a moderate correlation had a  $\rho$ -value between 0.4 and 0.7; and a  $\rho$ -value  $< 0.4$  was considered a weak association [61]. To determine if the difference between the correlations for unnormalized and any normalized data was significant, the `corr.test()` function was used to identify non-overlapping 95% confidence intervals (Cis).

### 3. Results

#### 3.1. Wastewater Treatment Plants

In the five utilities in the statewide monitoring, both N1 and N2 SARS-CoV-2 concentrations had moderately strong, significant correlations with 7-day moving average case data for individual sites and all pooled sites (Figure 1). Eaton WTTT had the weakest correlation but also had the smallest sample size (Table 1). Normalizing by population per utility, by definition, had no impact on correlations. In the pooled dataset, normalizing by population increased the correlation, but the difference was not significant compared to case data that was not population normalized. Spearman's  $\rho$  for Beaver Creek WRRF, Oxford WTTT, and Tri-Cities NR WTTT very slightly differ from Ma et al., 2022 [11] because the research presented here covers a longer time period and only includes data quantified by duplex RT-qPCR.

All Spearman's  $\rho$  correlation coefficients for all pooled sites between SARS-CoV-2, whether unnormalized or normalized, regardless of case data calculation, were significant ( $p$ -values  $< 0.05$ ) (Table S3). Normalizing SARS-CoV-2 gene concentrations by wastewater quality parameters alone through division or multiplication slightly improved the correlation to case data (Figure 2a,b), but the increase in Spearman's  $\rho$  was less than 0.05 and not statistically significant. Normalizing by flow and then other water quality parameters significantly improved the correlation between SARS-CoV-2 concentrations and the 7-day moving average (Figure 2c,d, Table S3). Both multiplying and dividing the flow normalized SARS-CoV-2 concentration by pH and temperature significantly improved correlations. For total suspended solids, both dividing and multiplying improved the correlation, but the difference between unnormalized and normalized by flow was only significant for multiplying by total suspended solids.

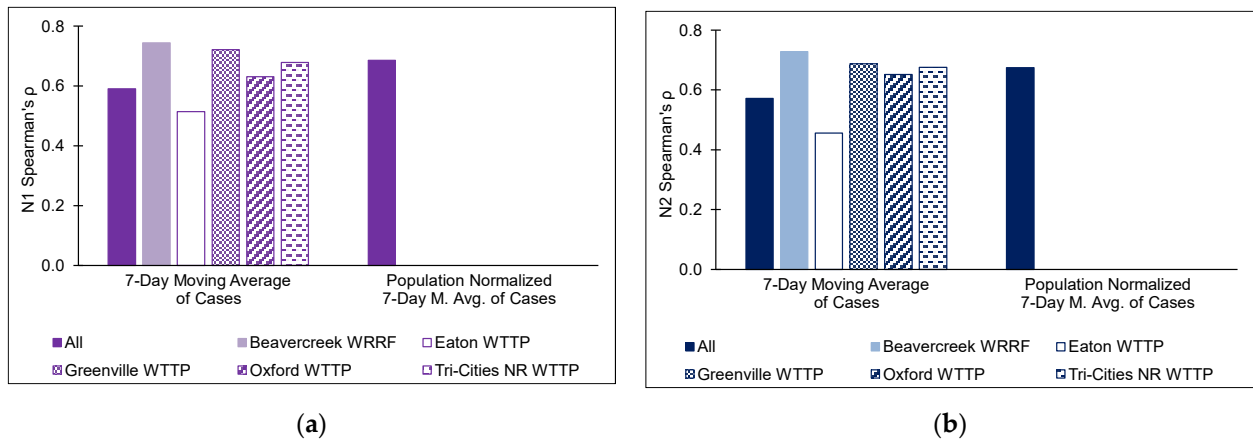


**Figure 1.** (a) Spearman’s  $\rho$  correlation coefficient between unnormalized SARS-CoV-2 N1 concentration and the 7-day moving average of COVID-19 cases for each individual WWTP and all pooled together (All). (b) Spearman’s  $\rho$  correlation coefficient between unnormalized SARS-CoV-2 N2 concentration and the 7-day moving average of COVID-19 cases for each individual WWTP and all pooled together (All).

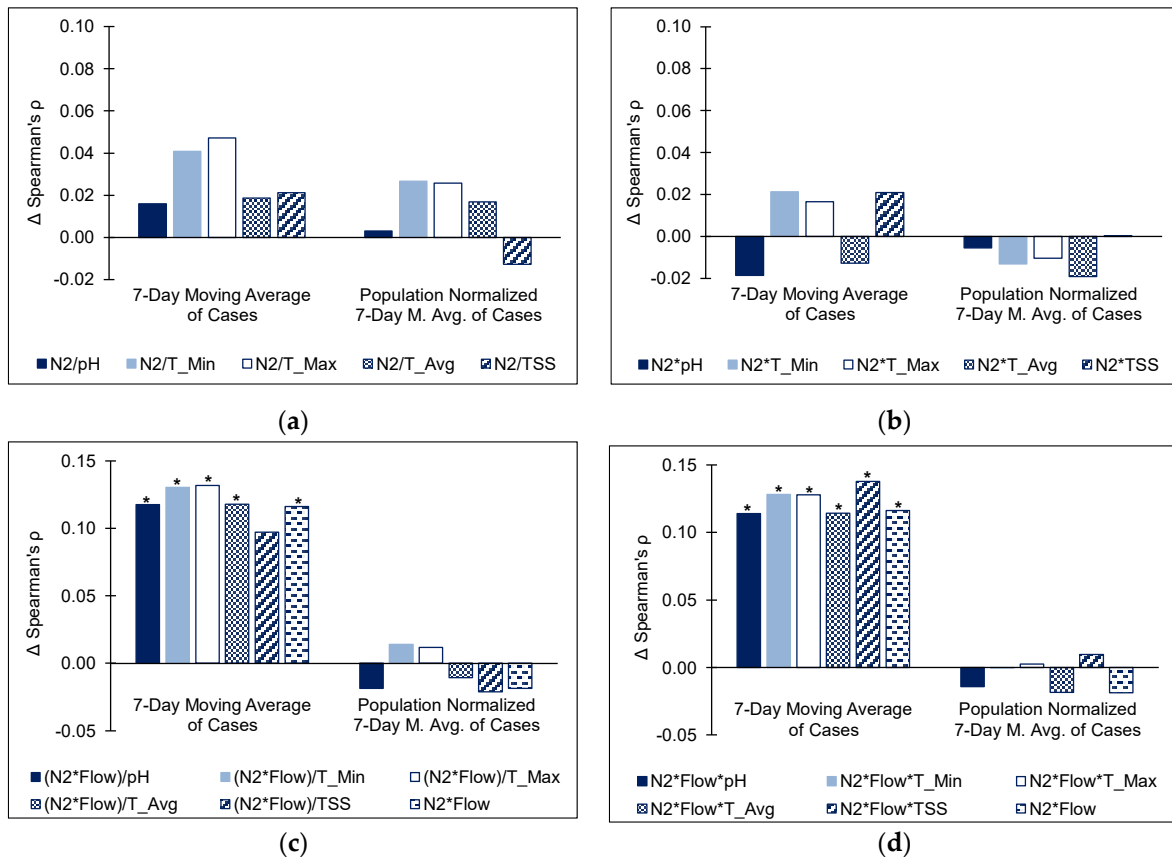


**Figure 2.** The difference ( $\Delta$ ) between Spearman’s  $\rho$  correlation coefficient for unnormalized N2 SARS-CoV-2 concentration and COVID-19 cases compared to Spearman’s  $\rho$  for normalized N2 SARS-CoV-2 concentration, normalized through (a) dividing it by water quality parameters; (b) multiplying it by water quality parameters; (c) multiplying by flow and then dividing by water quality parameters; and (d) multiplying by flow and then multiplying by water quality parameters. Asterisks on bars (\*) denote that the difference in Spearman’s  $\rho$  for unnormalized and normalized SARS-CoV-2 are significant based on non-overlapping 95% CIs.

Flow normalization did not improve SARS-CoV-2 concentration correlations to 7-day moving average case data when normalized by static population numbers. The difference in Spearman's  $\rho$  between unnormalized SARS-CoV-2 concentration and any normalized SARS-CoV-2 concentration between population normalized cases and the 7-day moving average was always less than 0.05 and never statistically significant.

Normalizing SARS-CoV-2 N1 and N2 by PMMoV but without flow normalization always significantly decreased the correlations to all four variations of case data (Table S3). With both flow and PMMoV normalization of SARS-CoV-2, Spearman's  $\rho$  also decreased in every normalization variation with water quality data compared to the unnormalized SARS-CoV-2, but the differences were not statistically significant (Table S3). Since Eaton WWTP did not provide TSS and minimum and maximum temperature data, the same pooled statistical analysis was done across all utilities except Eaton WWTP. Results showed the same trends, but the significance of difference decreased slightly, as expected, due to decreasing the sample size.

When analyzing utility data individually, PMMoV normalization of both SARS-CoV-2, with or without further water quality normalization, significantly decreased the correlation to the 7-day moving average of cases for all utilities (Tri-Cities was only significant for N1). The notable exception was Eaton, where flow normalization slightly decreased the correlation while PMMoV normalization slightly increased the correlation; however, the difference was insignificant for all normalizations.

For Beaver Creek WRRF, none of the normalizations of SARS-CoV-2 N2 increased Spearman's  $\rho$  to the 7-day moving average of cases compared to unnormalized SARS-CoV-2. For N1, multiplying by any of the temperatures on their own or with flow normalization slightly increased Spearman's  $\rho$  compared to unnormalized N1, but the change was insignificant (Table S4). For Eaton WWTP, normalizing SARS-CoV-2 N1 and N2 by pH or the average temperature showed small but insignificant improvement of Spearman's  $\rho$  correlation to the 7-day moving average of cases (Table S5). For Greenville WWTP, normalizing by dividing SARS-CoV-2 N1 and N2 by temperature and/or flow slightly improved correlations to the 7-day moving average of cases, but the change was insignificant (Table S6). For Oxford WWTP, normalizing by dividing SARS-CoV-2 N1 and N2 by temperature and/or flow slightly improved correlations to the 7-day moving average of cases, but the change was insignificant (Table S7). For Tri-Cities NR WWTP, none of the normalizations of SARS-CoV-2 N1 and N2 increased Spearman's  $\rho$  to the 7-day moving average of cases compared to unnormalized SARS-CoV-2 (Table S8).

### 3.2. Campus University Samples

Correlations between SARS-CoV-2 concentrations and the 7-day moving average case data on campus were very similar between all three genes (N1, N2, and E) and were moderate but not statistically significant (Figure 3, Table S9), in close alignment with previous analyses of these data [9]. Even though the difference between Spearman's  $\rho$  for unnormalized and many normalized SARS-CoV-2 concentrations increased by more than 0.2 (Figure 4), the difference was never statistically significant (Table S9), likely due to the small sample size. Spearman's  $\rho$  became statistically significant, however, when SARS-CoV-2 was divided or multiplied by E2:E3 and E2:E4 ratios (Figure 4a and Table S9).

When SARS-CoV-2 was normalized by PMMoV, the Spearman's  $\rho$  correlation coefficient to case data became significant for all three genes (Table S10), as were almost all further normalizations with water quality. Only a few normalizations further increased the correlation after PMMoV normalization of SARS-CoV-2 (Figure 4b). This included multiplying by electrical conductivity and UV absorbance ratios or dividing by SUVA.

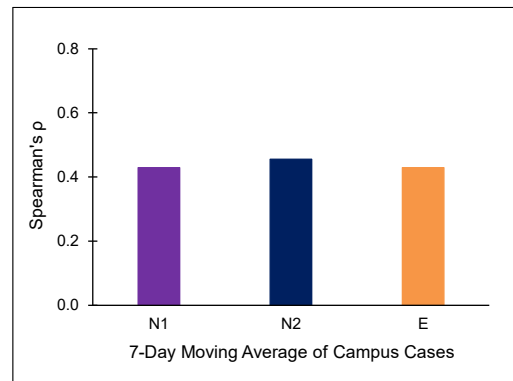


**Figure 3.** Spearman's  $\rho$  correlation coefficient for unnormalized SARS-CoV-2 N1, N2, and E gene concentrations and 7-day moving average COVID-19 cases for OSU campus data.

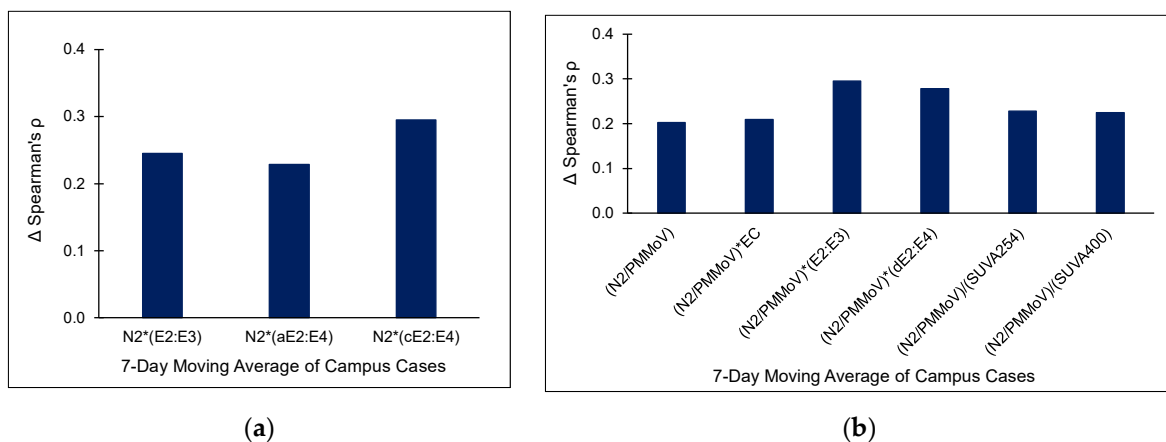


**Figure 4.** The difference between Spearman's  $\rho$  for unnormalized SARS-CoV-2 N2 concentrations and COVID-19 cases to Spearman's  $\rho$  for normalized SARS-CoV-2 N2 concentration, normalized through (a) multiplying it by water quality parameters and (b) dividing N2 by PMMoV and then performing further normalizations. See Table S1 for wavelengths of absorbance ratios.

**4. Discussion**

The COVID-19 pandemic drove an increase in the use of WBE, and it is still used for continued COVID-19 monitoring in addition to other pathogens and/or pharmaceuticals. To achieve the maximum benefit from WBE, measured concentrations need to correlate with relevant epidemiological parameters, represent specific changes in pathogen prevalence in variable wastewater conditions, and be reported in a standardized manner [62]. Additionally, the difference in correlations between cases and SARS-CoV-2 in wastewater in large communities and small communities needs to be understood. Populations in certain communities can fluctuate significantly, and specific habits in some communities can also lead to a lower likelihood of getting clinical testing. Normalizing SARS-CoV-2 by a parameter that estimates population, such as mobile device data [8,13], ammonia [63], human fecal strength [9,21], or flow, is needed to compare across different temporal and spatial scales [2,7,14].

Accounting for flow, pH, temperature, and total suspended solids strengthened correlations for SARS-CoV-2 N1 and N2 to COVID-19 cases for pooled wastewater treatment plants, which agrees with other studies [3,15]. The pH, temperature, and solids content of wastewater can impact the genetic material of SARS-CoV-2 and decrease detection [29]. Therefore, multiplying SARS-CoV-2 concentrations by these parameters increased the correlation to case data, as the multiplication adjusts for higher parameter values decreasing SARS-CoV-2 in wastewater. PMMoV normalization was not useful for improving WBE correlations here in 24 h composite samples from wastewater treatment plants. Composite

samples for influent wastewater for communities greater than 10,000 people likely do not need PMMoV normalization as PMMoV does not correspond well to sewershed size and population served in larger systems [3,16] where flow quality is likely to be more consistent. The only utility that showed any (but still insignificant) improvement by PMMoV normalization was the utility serving the smallest population, close to 10,000. These results are supported by multiple studies that find PMMoV normalization of SARS-CoV-2 inadequate in improving WBE data [3,7,10,14] but contradict some that recommend PMMoV normalization for large populations [20,21]. Flow, which improved correlations here and in other studies [3,64], can help capture the dynamic nature of the population contributing to the WTP. Flow normalization was less effective when performed on data from individual WWTPs, likely due to decreased flow fluctuations in a large sewershed, which agrees with another study [65], especially considering that the composite samples were taken at the same time and day every week. Discontinuing measurement of PMMoV for moderate to large WTPs would reduce costs [3,11] drastically for large scale networks performing WBE (such as the Ohio Coronavirus Wastewater Monitoring Network), especially since flow, pH, and temperature are already measured as part of routine monitoring by WTPs.

For the campus data, as previously reported, the turbidity, pH, and total suspended solids water quality data alone had no correlation to SARS-CoV-2 N1, N2, and E gene concentrations (all Spearman's  $\rho$  correlation coefficients  $< 0.4$ ) [9]. However, using the water quality data to normalize SARS-CoV-2 improved correlations to case data. In this campus study, PMMoV normalization was crucial for increasing correlations of SARS-CoV-2 to the 7-day moving average. Grab samples, especially ones close to their source, only capture a small snapshot of the flow in a sewer. PMMoV normalization has been shown to be suitable for normalizing SARS-CoV-2 data from small sewersheds or grab samples [16]. Additionally, while total suspended solids, total coliform, and *E. coli* are common indicators for wastewater strength [24,25], normalization with their concentrations did not aid correlations, in agreement with another study [16]. However, normalizations with some of the UV absorbance parameters (SUVA or UV ratios) did improve correlations. Another study investigated if UV absorbance was associated with SARS-CoV-2 detection [43], but this is the first study to report that normalization with UV absorbance characteristics can improve the relationship of SARS-CoV-2 to COVID-19 case data. Although SUVA and UV ratios are not a direct measure of fecal strength, they do characterize the composition of the dissolved organic carbon present in the wastewater [38]. Additionally, UV absorption values can vary from the wastewater norm due to surfactants and other contaminants, including personal care products [66]. Because the grab samples from campus are incredibly variable each week and manholes served dorms, gyms, and cafeterias that could contribute varying amounts of non-fecal wastewater, it is possible that UV absorption characteristics best adjust for those differences. Measuring UV absorbance is quicker and requires fewer consumables than biological culture or nucleic acid measurements. It is possible that some of the parameters in campus monitoring, such as total suspended solids, would have a stronger normalization impact if samples were 24 h composite samples. SARS-CoV-2 can attach to solids particles, and therefore TSS content can have a different impact on SARS-CoV-2 extraction whether the centrifugation method or ultrafiltration method is used, which TSS normalization could help resolve [43].

In addition to the complexity of comparing results from grab samples to 24 h composite samples, the temperature of the campus samples was considerably warmer than the WWTP influent flow. Warm temperatures are known to degrade SARS-CoV-2 faster than cooler temperatures [33–36], but the low hydraulic retention time and immediate transport on ice of the grab samples in the campus sewer should have minimized temperature impacts [37], especially in comparison to longer travel times to wastewater treatment plants. Another important difference between the two sample types was that the WWTP samples were quantified with RT-qPCR while the campus samples were quantified with ddPCR, with ddPCR being more sensitive to SARS-CoV-2, which is especially important when there is low viral load in the wastewater [67,68].

Some of the limitations include that while on-campus students were required to test twice a week, only 60% of the student population was sampled through the sewer wastewater data. Due to Health Insurance Portability and Accountability Act (HIPAA) regulations, we were unable to get positive cases for specific buildings that contributed to a manhole sample location. This can skew results if cases were spreading in specific dormitories that were not sampled. Cases linked to WWTP sewersheds came from voluntary clinical testing, which may not capture all positive cases, especially as at-home tests became available [65]. Additionally, humans shed a variable amount of SARS-CoV-2 in their feces, ranging from  $10^2$ – $10^7$  gene copies/mL [45]. The virus can be shed in the stool before symptoms appear, providing a possible lead time where SARS-CoV-2 is detected before positive cases are reported [2]. Most studies use moving averages to account for the lag in positive cases compared to detection of SARS-CoV-2 in the wastewater or model a lead time, but lead times and best moving average values can vary across different sewersheds [65,69]. This study only tested a 7-day moving average and without modeling any lead times.

Depending on the type of sample and the size and characteristics of the population in the sewershed, different normalization methods should be utilized. This study finds that PMMoV normalization of SARS-CoV-2 from wastewater treatment plants serving more than 10,000 people is not necessary, and that flow and other physicochemical parameters that are part of routine monitoring are suitable for SARS-CoV-2 normalization to increase WBE correlation and decrease analytical time and cost. For grab samples in campus-scale sewersheds, and possibly in composite samples from small sewersheds, correcting for human fecal strength, either through PMMoV normalization or a parameter that provides information about the structure and composition of the solids, such as DOC, UV absorbance ratios, or SUVA, is critical. This will improve trend analysis for WBE.

**Supplementary Materials:** The following supporting information can be downloaded at: <https://www.mdpi.com/article/10.3390/environments11040080/s1>, Table S1: UV absorbance ratios; Table S2: Average wastewater parameters for campus sites; Equations (S1)–(S128): Normalizations of SARS-CoV-2 gene concentration; Table S3: Spearman's  $\rho$  for SARS-CoV-2 N1 and N2 and COVID-19 cases for all WTPs pooled together; Table S4: Spearman's  $\rho$  for SARS-CoV-2 N1 and N2 and COVID-19 cases for Beavercreek WRRF; Table S5: Spearman's  $\rho$  for SARS-CoV-2 N1 and N2 and COVID-19 cases for Eaton WTP; Table S6: Spearman's  $\rho$  for SARS-CoV-2 N1 and N2 and COVID-19 cases for Greenville WTP; Table S7: Spearman's  $\rho$  for SARS-CoV-2 N1 and N2 and COVID-19 cases for Oxford WTP; Table S8: Spearman's  $\rho$  for SARS-CoV-2 N1 and N2 and COVID-19 cases for Tri-Cities NR WTP; Table S9: Spearman's  $\rho$  for SARS-CoV-2 N1,N2, and E and COVID-19 cases for the campus data; Table S10: Spearman's  $\rho$  for PMMoV normalized SARS-CoV-2 N1,N2, and E and COVID-19 cases for the campus data.

**Author Contributions:** Conceptualization, J.S. and N.M.H.; methodology, J.S. and N.M.H.; validation, J.S. and N.M.H.; formal analysis, J.S.; investigation, J.S.; resources, N.M.H.; data curation, J.S.; writing—original draft preparation, J.S.; writing—review and editing, N.M.H.; visualization, J.S.; supervision, N.M.H.; project administration, N.M.H.; funding acquisition, N.M.H. All authors have read and agreed to the published version of the manuscript.

**Funding:** For the wastewater treatment utilities research portion, this research was funded by the Ohio Environmental Protection Agency through the United States Environmental Protection Agency Coronavirus Aid, Relief, and Economic Security (CARES) Act project number OSU-FDCARES20, and the Ohio Department of Health through the Center for Disease Control and Prevention (CDC) award number 6 NU50CK000543-02-11. For The Ohio State University campus research portion, this research was funded by the Ohio Department of Health and the Ohio State University (Contact Tracing and Comprehensive Monitoring Team Programs).

**Data Availability Statement:** For the wastewater treatment plant research presented in this paper, data are publicly available at <https://data.ohio.gov/wps/portal/gov/data/view/covid-19-reporting> (accessed on 1 May 2023). For the campus research presented in this paper, COVID-19 case data are available at the archived link <https://safeandhealthy.osu.edu/dashboard> (accessed on 1 May 2023). Molecular campus data can be supplied upon reasonable request.

**Acknowledgments:** We thank Jiyoung Lee and her research group for providing the campus molecular and COVID-19 case data.

**Conflicts of Interest:** The authors declare no conflicts of interest.

## References

1. Adhikari, S.; Halden, R.U. Opportunities and limits of wastewater-based epidemiology for tracking global health and attainment of UN sustainable development goals. *Environ. Int.* **2022**, *163*, 107217. [[CrossRef](#)]
2. Daughton, C.G. Wastewater surveillance for population-wide COVID-19: The present and future. *Sci. Total Environ.* **2020**, *736*, 139631. [[CrossRef](#)]
3. Maal-Bared, R.; Qiu, Y.; Li, Q.; Gao, T.; Hruday, S.E.; Bhavanam, S.; Ruecker, N.J.; Ellehoj, E.; Lee, B.E.; Pang, X. Does normalization of SARS-CoV-2 concentrations by Pepper Mild Mottle Virus improve correlations and lead time between wastewater surveillance and clinical data in Alberta (Canada): Comparing twelve SARS-CoV-2 normalization approaches. *Sci. Total Environ.* **2023**, *856*, 158964. [[CrossRef](#)]
4. Mazumder, P.; Dash, S.; Honda, R.; Sonne, C.; Kumar, M. Sewage surveillance for SARS-CoV-2: Molecular detection, quantification, and normalization factors. *Curr. Opin. Environ. Sci. Health* **2022**, *28*, 100363. [[CrossRef](#)]
5. Arabzadeh, R.; Grünbacher, D.M.; Insam, H.; Kreuzinger, N.; Markt, R.; Rauch, W. Data filtering methods for SARS-CoV-2 wastewater surveillance. *Water Sci. Technol.* **2021**, *84*, 1324–1339. [[CrossRef](#)]
6. Wade, M.J.; Jacomo, A.L.; Armenise, E.; Brown, M.R.; Bunce, J.T.; Cameron, G.J.; Fang, Z.; Farkas, K.; Gilpin, D.F.; Graham, D.W.; et al. Understanding and managing uncertainty and variability for wastewater monitoring beyond the pandemic: Lessons learned from the United Kingdom national COVID-19 surveillance programmes. *J. Hazard. Mater.* **2022**, *424 Pt B*, 127456. [[CrossRef](#)]
7. Greenwald, H.D.; Kennedy, L.C.; Hinkle, A.; Whitney, O.N.; Fan, V.B.; Crits-Christoph, A.; Harris-Lovett, S.; Flamholz, A.I.; Al-Shayeb, B.; Liao, L.D.; et al. Tools for interpretation of wastewater SARS-CoV-2 temporal and spatial trends demonstrated with data collected in the San Francisco Bay Area. *Water Res. X* **2021**, *12*, 100111. [[CrossRef](#)]
8. Sim, W.; Park, S.; Ha, J.; Kim, D.; Oh, J.-E. Evaluation of population estimation methods for wastewater-based epidemiology in a metropolitan city. *Sci. Total Environ.* **2023**, *857*, 159154. [[CrossRef](#)]
9. Lu, E.; Ai, Y.; Davis, A.; Straathof, J.; Halloran, K.; Hull, N.; Winston, R.; Weir, M.H.; Soller, J.; Bohrerova, Z.; et al. Wastewater surveillance of SARS-CoV-2 in dormitories as a part of comprehensive university campus COVID-19 monitoring. *Environ. Res.* **2022**, *212*, 113580. [[CrossRef](#)]
10. Ai, Y.; Davis, A.; Jones, D.; Lemeshow, S.; Tu, H.; He, F.; Ru, P.; Pan, X.; Bohrerova, Z.; Lee, J. Wastewater SARS-CoV-2 monitoring as a community-level COVID-19 trend tracker and variants in Ohio, United States. *Sci. Total Environ.* **2021**, *801*, 149757. [[CrossRef](#)]
11. Ma, D.; Straathof, J.; Liu, Y.; Hull, N.M. Monitoring SARS-CoV-2 RNA in Wastewater with RT-qPCR and Chip-Based RT-dPCR: Sewershed-Level Trends and Relationships to COVID-19. *ACS EST Water* **2022**, *2*, 2084–2093. [[CrossRef](#)]
12. Castiglioni, S.; Bijlsma, L.; Covaci, A.; Emke, E.; Hernández, F.; Reid, M.; Ort, C.; Thomas, K.V.; van Nuijs, A.L.N.; de Voogt, P.; et al. Evaluation of Uncertainties Associated with the Determination of Community Drug Use through the Measurement of Sewage Drug Biomarkers. *Environ. Sci. Technol.* **2013**, *47*, 1452–1460. [[CrossRef](#)]
13. Baz-Lomba, J.A.; Di Ruscio, F.; Amador, A.; Reid, M.; Thomas, K.V. Assessing Alternative Population Size Proxies in a Wastewater Catchment Area Using Mobile Device Data. *Environ. Sci. Technol.* **2019**, *53*, 1994–2001. [[CrossRef](#)]
14. Feng, S.; Roguet, A.; McClary-Gutierrez, J.S.; Newton, R.J.; Kloczko, N.; Meiman, J.G.; McLellan, S.L. Evaluation of Sampling, Analysis, and Normalization Methods for SARS-CoV-2 Concentrations in Wastewater to Assess COVID-19 Burdens in Wisconsin Communities. *ACS EST Water* **2021**, *1*, 1955–1965. [[CrossRef](#)]
15. Sakarovich, C.; Schlosser, O.; Courtois, S.; Proust-Lima, C.; Couallier, J.; Pétrau, A.; Litrico, X.; Loret, J.-F. Monitoring of SARS-CoV-2 in wastewater: What normalisation for improved understanding of epidemic trends? *J. Water Health* **2022**, *20*, 712–726. [[CrossRef](#)]
16. Zhan, Q.; Babler, K.M.; Sharkey, M.E.; Amirali, A.; Beaver, C.C.; Boone, M.M.; Comerford, S.; Cooper, D.; Cortizas, E.M.; Currall, B.B.; et al. Relationships between SARS-CoV-2 in Wastewater and COVID-19 Clinical Cases and Hospitalizations, with and without Normalization against Indicators of Human Waste. *ACS EST Water* **2022**, *2*, 1992–2003. [[CrossRef](#)]
17. Jarret, R.L.; Gillaspie, A.G.; Barkley, N.A.; Pinnow, D.L. The Occurrence and Control of Pepper Mild Mottle Virus (PMMoV) in the USDA/ARS Capsicum Germplasm Collection. *Seed Technol.* **2008**, *30*, 26–36.
18. Peng, J.; Shi, B.; Zheng, H.; Lu, Y.; Lin, L.; Jiang, T.; Chen, J.; Yan, F. Detection of pepper mild mottle virus in pepper sauce in China. *Arch. Virol.* **2015**, *160*, 2079–2082. [[CrossRef](#)]
19. Zhou, W.P.; Li, Y.Y.; Li, F.; Tan, G.L. First report of natural infection of tomato by pepper mild mottle virus in China. *J. Plant Pathol.* **2021**, *103*, 363. [[CrossRef](#)]
20. D’Aoust, P.M.; Graber, T.E.; Mercier, E.; Montpetit, D.; Alexandrov, I.; Neault, N.; Baig, A.T.; Mayne, J.; Zhang, X.; Alain, T.; et al. Catching a resurgence: Increase in SARS-CoV-2 viral RNA identified in wastewater 48 h before COVID-19 clinical tests and 96 h before hospitalizations. *Sci. Total Environ.* **2021**, *770*, 145319. [[CrossRef](#)]
21. Nagarkar, M.; Keely, S.; Jahne, M.; Wheaton, E.; Hart, C.; Smith, B.; Garland, J.; Varughese, E.; Braam, A.; Wiechman, B.; et al. SARS-CoV-2 monitoring at three sewersheds of different scales and complexity demonstrates distinctive relationships between wastewater measurements and COVID-19 case data. *Sci. Total Environ.* **2022**, *816*, 151534. [[CrossRef](#)]

22. Greaves, J.; Stone, D.; Wu, Z.; Bibby, K. Persistence of emerging viral fecal indicators in large-scale freshwater mesocosms. *Water Res. X* **2020**, *9*, 100067. [[CrossRef](#)]
23. LaTurner, Z.W.; Zong, D.M.; Kalvapalle, P.; Gamas, K.R.; Terwilliger, A.; Crosby, T.; Ali, P.; Avadhanula, V.; Santos, H.H.; Weesner, K.; et al. Evaluating recovery, cost, and throughput of different concentration methods for SARS-CoV-2 wastewater-based epidemiology-PMC. *Water Res.* **2021**, *197*, 117043. [[CrossRef](#)]
24. Glassmeyer, S.T.; Furlong, E.T.; Kolpin, D.W.; Cahill, J.D.; Zaugg, S.D.; Werner, S.L.; Meyer, M.T.; Kryak, D.D. Transport of Chemical and Microbial Compounds from Known Wastewater Discharges: Potential for Use as Indicators of Human Fecal Contamination. *Environ. Sci. Technol.* **2005**, *39*, 5157–5169. [[CrossRef](#)]
25. Sankararamkrishnan, N.; Guo, Q. Chemical tracers as indicator of human fecal coliforms at storm water outfalls. *Environ. Int.* **2005**, *31*, 1133–1140. [[CrossRef](#)]
26. Ahmed, W.; Bertsch, P.M.; Bibby, K.; Haramoto, E.; Hewitt, J.; Huygens, F.; Gyawali, P.; Korajkic, A.; Riddell, S.; Sherchan, S.P.; et al. Decay of SARS-CoV-2 and surrogate murine hepatitis virus RNA in untreated wastewater to inform application in wastewater-based epidemiology. *Environ. Res.* **2020**, *191*, 110092. [[CrossRef](#)]
27. Yang, S.; Dong, Q.; Li, S.; Cheng, Z.; Kang, X.; Ren, D.; Xu, C.; Zhou, X.; Liang, P.; Sun, L.; et al. Persistence of SARS-CoV-2 RNA in wastewater after the end of the COVID-19 epidemics. *J. Hazard. Mater.* **2022**, *429*, 128358. [[CrossRef](#)]
28. Achak, M.; Bakri, S.A.; Chhiti, Y.; Alaoui, F.E.M.; Barka, N.; Boumya, W. SARS-CoV-2 in hospital wastewater during outbreak of COVID-19: A review on detection, survival and disinfection technologies. *Sci. Total Environ.* **2021**, *761*, 143192. [[CrossRef](#)]
29. Hamouda, M.; Mustafa, F.; Maraqa, M.; Rizvi, T.; Hassan, A.A. Wastewater surveillance for SARS-CoV-2: Lessons learnt from recent studies to define future applications. *Sci. Total Environ.* **2021**, *759*, 143493. [[CrossRef](#)]
30. Casanova, L.; Rutala, W.A.; Weber, D.J.; Sobsey, M.D. Survival of surrogate coronaviruses in water. *Water Res.* **2009**, *43*, 1893–1898. [[CrossRef](#)]
31. Amoah, I.D.; Abunama, T.; Awolusi, O.O.; Pillay, L.; Pillay, K.; Kumari, S.; Bux, F. Effect of selected wastewater characteristics on estimation of SARS-CoV-2 viral load in wastewater. *Environ. Res.* **2022**, *203*, 111877. [[CrossRef](#)]
32. Sapula, S.A.; Whittall, J.J.; Pandopoulos, A.J.; Gerber, C.; Venter, H. An optimized and robust PEG precipitation method for detection of SARS-CoV-2 in wastewater. *Sci. Total Environ.* **2021**, *785*, 147270. [[CrossRef](#)]
33. Schussman, M.K.; McLellan, S.L. Effect of Time and Temperature on SARS-CoV-2 in Municipal Wastewater Conveyance Systems. *Water* **2022**, *14*, 1373. [[CrossRef](#)]
34. Guo, Y.; Liu, Y.; Gao, S.; Zhou, X.; Sivakumar, M.; Jiang, G. Effects of Temperature and Water Types on the Decay of Coronavirus: A Review. *Water* **2023**, *15*, 1051. [[CrossRef](#)]
35. Bivins, A.; Greaves, J.; Fischer, R.; Yinda, K.C.; Ahmed, W.; Kitajima, M.; Munster, V.J.; Bibby, K. Persistence of SARS-CoV-2 in Water and Wastewater. *Environ. Sci. Technol. Lett.* **2020**, *7*, 937–942. [[CrossRef](#)]
36. de Oliveira, L.C.; Torres-Franco, A.F.; Lopes, B.C.; Santos, B.S.d.S.; Costa, E.A.; Costa, M.S.; Reis, M.T.P.; Melo, M.C.; Polizzi, R.B.; Teixeira, M.M.; et al. Viability of SARS-CoV-2 in river water and wastewater at different temperatures and solids content. *Water Res.* **2021**, *195*, 117002. [[CrossRef](#)]
37. Weidhaas, J.; Aanderud, Z.T.; Roper, D.K.; VanDerslice, J.; Gaddis, E.B.; Ostermiller, J.; Hoffman, K.; Jamal, R.; Heck, P.; Zhang, Y.; et al. Correlation of SARS-CoV-2 RNA in wastewater with COVID-19 disease burden in sewersheds. *Sci. Total Environ.* **2021**, *775*, 145790. [[CrossRef](#)]
38. Peacock, M.; Evans, C.D.; Fenner, N.; Freeman, C.; Gough, R.; Jones, T.G.; Lebron, I. UV-visible absorbance spectroscopy as a proxy for peatland dissolved organic carbon (DOC) quantity and quality: Considerations on wavelength and absorbance degradation. *Environ. Sci. Process. Impacts* **2014**, *16*, 1445–1461. [[CrossRef](#)]
39. Altmann, J.; Massa, L.; Sperlich, A.; Gnirss, R.; Jekel, M. UV254 absorbance as real-time monitoring and control parameter for micropollutant removal in advanced wastewater treatment with powdered activated carbon. *Water Res.* **2016**, *94*, 240–245. [[CrossRef](#)]
40. Mesquita, D.P.; Quintelas, C.; Amaral, A.L.; Ferreira, E.C. Monitoring biological wastewater treatment processes: Recent advances in spectroscopy applications. *Rev. Environ. Sci. Biotechnol.* **2017**, *16*, 395–424. [[CrossRef](#)]
41. Waltham, B.; Örmeci, B. Fluorescence intensity, conductivity, and UV-vis absorbance as surrogate parameters for real-time monitoring of anaerobic digestion of wastewater sludge. *J. Water Proc. Eng.* **2020**, *37*, 101395. [[CrossRef](#)]
42. Ulliman, S.L.; Korak, J.A.; Linden, K.G.; Rosario-Ortiz, F.L. Methodology for selection of optical parameters as wastewater effluent organic matter surrogates. *Water Res.* **2020**, *170*, 115321. [[CrossRef](#)]
43. Bitter, L.C.; Kibbee, R.; Jiménez, G.C.; Örmeci, B. Wastewater Surveillance of SARS-CoV-2 at a Canadian University Campus and the Impact of Wastewater Characteristics on Viral RNA Detection. *ACS EST Water* **2022**, *2*, 2034–2046. [[CrossRef](#)] [[PubMed](#)]
44. Carvalho, M.C.; Eyre, B.D. A low cost, easy to build, portable, and universal autosampler for liquids. *Methods Oceanogr.* **2013**, *8*, 23–32. [[CrossRef](#)]
45. Jones, D.L.; Baluja, M.Q.; Graham, D.W.; Corbishley, A.; McDonald, J.E.; Malham, S.K.; Hillary, L.S.; Connor, T.R.; Gaze, W.H.; Moura, I.B.; et al. Shedding of SARS-CoV-2 in feces and urine and its potential role in person-to-person transmission and the environment-based spread of COVID-19. *Sci. Total Environ.* **2020**, *749*, 141364. [[CrossRef](#)] [[PubMed](#)]
46. Duvallet, C.; Wu, F.; McElroy, K.A.; Imakaev, M.; Endo, N.; Xiao, A.; Zhang, J.; Floyd-O’Sullivan, R.; Powell, M.M.; Mendola, S.; et al. Nationwide Trends in COVID-19 Cases and SARS-CoV-2 RNA Wastewater Concentrations in the United States. *ACS EST Water* **2022**, *2*, 1899–1909. [[CrossRef](#)] [[PubMed](#)]

47. Bohrerova, Z.; Brinkman, N.E.; Chakravarti, R.; Chattopadhyay, S.; Faith, S.A.; Garland, J.; Herrin, J.M.; Hull, N.; Jahne, M.; Kang, D.-W.; et al. Ohio Coronavirus Wastewater Monitoring Network: Implementation of Statewide Monitoring for Protecting Public Health. *J. Public Health Manag. Pract.* **2023**, *29*, 845–853. [[CrossRef](#)] [[PubMed](#)]
48. Ohio Department of Health. Ohio Wastewater Monitoring Network Sample Results. Available online: <https://data.ohio.gov/wps/portal/gov/data/view/ohio-wastewater-monitoring-network-sample-results> (accessed on 17 February 2024).
49. Weishaar, J.L.; Aiken, G.R.; Bergamaschi, B.A.; Fram, M.S.; Fujii, R.; Mopper, K. Evaluation of specific ultraviolet absorbance as an indicator of the chemical composition and reactivity of dissolved organic carbon. *Environ. Sci. Technol.* **2003**, *37*, 4702–4708. [[CrossRef](#)] [[PubMed](#)]
50. Duirk, S.E.; Valentine, R.L. Modeling dichloroacetic acid formation from the reaction of monochloramine with natural organic matter. *Water Res.* **2006**, *40*, 2667–2674. [[CrossRef](#)]
51. Worrall, F.; Armstrong, A.; Holden, J. Short-term impact of peat drain-blocking on water colour, dissolved organic carbon concentration, and water table depth. *J. Hydrol.* **2007**, *337*, 315–325. [[CrossRef](#)]
52. Peuravuori, J.; Pihlaja, K. Molecular size distribution and spectroscopic properties of aquatic humic substances. *Anal. Chim. Acta* **1997**, *337*, 133–149. [[CrossRef](#)]
53. Graham, M.C.; Gavin, K.G.; Kirika, A.; Farmer, J.G. Processes controlling manganese distributions and associations in organic-rich freshwater aquatic systems: The example of Loch Bradan, Scotland. *Sci. Total Environ.* **2012**, *424*, 239–250. [[CrossRef](#)] [[PubMed](#)]
54. Selberg, A.; Viik, M.; Ehapalu, K.; Tenno, T. Content and composition of natural organic matter in water of Lake Pitkjärvi and mire feeding Kuke River (Estonia). *J. Hydrol.* **2011**, *400*, 274–280. [[CrossRef](#)]
55. Park, S.; Joe, K.S.; Han, S.H.; Kim, H.S. Characteristics of Dissolved Organic Carbon in the Leachate from Moonam Sanitary Landfill. *Environ. Technol.* **1999**, *20*, 419–424. [[CrossRef](#)]
56. Moore, T.R. A Preliminary Study of the Effects of Drainage and Harvesting on Water Quality in Ombrotrophic Bogs Near Sept-Iles, Quebec. *J. Am. Water Resour. Assoc.* **1987**, *23*, 785–791. [[CrossRef](#)]
57. Wilson, L.; Wilson, J.; Holden, J.; Johnstone, I.; Armstrong, A.; Morris, M. Ditch blocking, water chemistry and organic carbon flux: Evidence that blanket bog restoration reduces erosion and fluvial carbon loss. *Sci. Total Environ.* **2011**, *409*, 2010–2018. [[CrossRef](#)] [[PubMed](#)]
58. Thurman, E.M. *Organic Geochemistry of Natural Waters*; Martinus Nijhoff/Dr W. Junk Publishers: Dordrecht, The Netherlands, 1985.
59. Wallage, Z.E.; Holden, J.; McDonald, A.T. Drain blocking: An effective treatment for reducing dissolved organic carbon loss and water discolouration in a drained peatland. *Sci. Total Environ.* **2006**, *367*, 811–821. [[CrossRef](#)] [[PubMed](#)]
60. The Ohio State University. COVID-19 Dashboard (Archived). Safe and Healthy Buckeyes. Available online: <https://safeandhealthy.osu.edu/dashboard> (accessed on 18 February 2024).
61. von Sperling, M.; Verbyla, M.E.; Oliveira, S.M.A.C. *Assessment of Treatment Plant Performance and Water Quality Data: A Guide for Students, Researchers and Practitioners*; IWA Publishing: London, UK, 2020.
62. McClary-Gutierrez, J.S.; Mattioli, M.C.; Marcenac, P.; Silverman, A.I.; Boehm, A.B.; Bibby, K.; Balliet, M.; Reyes, F.L.d.L.; Gerrity, D.; Griffith, J.F.; et al. SARS-CoV-2 Wastewater Surveillance for Public Health Action. *Emerg. Infect. Dis.* **2021**, *27*, e210753. [[CrossRef](#)] [[PubMed](#)]
63. Been, F.; Rossi, L.; Ort, C.; Rudaz, S.; Delémont, O.; Esseiva, P. Population normalization with ammonium in wastewater-based epidemiology: Application to illicit drug monitoring. *Environ. Sci. Technol.* **2014**, *48*, 8162–8169. [[CrossRef](#)]
64. Sims, N.; Kasprzyk-Hordern, B. Future perspectives of wastewater-based epidemiology: Monitoring infectious disease spread and resistance to the community level. *Environ. Int.* **2020**, *139*, 105689. [[CrossRef](#)]
65. Schill, R.; Nelson, K.L.; Harris-Lovett, S.; Kantor, R.S. The dynamic relationship between COVID-19 cases and SARS-CoV-2 wastewater concentrations across time and space: Considerations for model training data sets. *Sci. Total Environ.* **2023**, *871*, 162069. [[CrossRef](#)] [[PubMed](#)]
66. Spangenberg, M.; Bryant, J.I.; Gibson, S.J.; Mousley, P.J.; Ramachers, Y.; Bell, G.R. Ultraviolet absorption of contaminants in water. *Sci. Rep.* **2021**, *11*, 3682. [[CrossRef](#)] [[PubMed](#)]
67. Li, J.; Lin, W.; Du, P.; Liu, W.; Liu, X.; Yang, C.; Jia, R.; Wang, Y.; Chen, Y.; Jia, L.; et al. Comparison of reverse-transcription qPCR and droplet digital PCR for the detection of SARS-CoV-2 in clinical specimens of hospitalized patients. *Diagn. Microbiol. Infect. Dis.* **2022**, *103*, 115677. [[CrossRef](#)] [[PubMed](#)]
68. Morón-López, S.; Riveira-Muñoz, E.; Urrea, V.; Gutiérrez-Chamorro, L.; Ávila-Nieto, C.; Noguera-Julian, M.; Carrillo, J.; Mitjà, O.; Mateu, L.; Massanella, M.; et al. Comparison of Reverse Transcription (RT)-Quantitative PCR and RT-Droplet Digital PCR for Detection of Genomic and Subgenomic SARS-CoV-2 RNA. *Microbiol. Spectr.* **2023**, *11*, e0415922. [[CrossRef](#)]
69. Olesen, S.W.; Imakaev, M.; Duvall, C. Making waves: Defining the lead time of wastewater-based epidemiology for COVID-19. *Water Res.* **2021**, *202*, 117433. [[CrossRef](#)]

**Disclaimer/Publisher’s Note:** The statements, opinions and data contained in all publications are solely those of the individual author(s) and contributor(s) and not of MDPI and/or the editor(s). MDPI and/or the editor(s) disclaim responsibility for any injury to people or property resulting from any ideas, methods, instructions or products referred to in the content.